

Finite-distance corrections to the gravitational bending angle of light in the strong deflection limit

Asahi Ishihara, Yusuke Suzuki, Toshiaki Ono, and Hideki Asada

Faculty of Science and Technology,

Hirosaki University, Aomori 036-8561, Japan

(Dated: January 26, 2017)

Abstract

Continuing work initiated in an earlier publication [Ishihara, Suzuki, Ono, Kitamura, Asada, Phys. Rev. D **94**, 084015 (2016)], we discuss a method of calculating the bending angle of light in a static, spherically symmetric and asymptotically flat spacetime, especially by taking account of the finite distance from a lens object to a light source and a receiver. For this purpose, we use the Gauss-Bonnet theorem to define the bending angle of light, such that the definition can be valid also in the strong deflection limit. Finally, this method is applied to Schwarzschild spacetime in order to discuss also possible observational implications. The proposed corrections for Sgr A* for instance are able to amount to $\sim 10^{-5}$ arcseconds for some parameter range, which may be within the capability of near-future astronomy, while also the correction for the Sun in the weak field limit is $\sim 10^{-5}$ arcseconds.

PACS numbers: 04.40.-b, 95.30.Sf, 98.62.Sb

I. INTRODUCTION

Since 1919 [1], experimental confirmations of the theory of general relativity [2] by measuring the gravitational bending of light by the Sun have been done. The gravitational bending of light by other astronomical objects has been observed at many times. The gravitational lensing has been well established as one of the powerful tools in astronomy and cosmology.

The gravitational bending of light plays an important role also in the theoretical study of gravity, for example on a null structure of a spacetime. Hagihara found the analytical solution for light trajectories in the gravitational field of Schwarzschild [3], where the expressions involve incomplete elliptic integrals of the first kind. See [4] for exact solutions for the light trajectory in Schwarzschild and some other black hole solutions. See e.g. [5, 6] for a review on the light deflection in the weak-field approximation of Schwarzschild spacetime. A generalized lens equation for the light deflection in Schwarzschild metric in the weak-field approximation and valid for finite distances of source and observer from the lens was discussed by Zschocke [7].

In order to understand a strong gravitational field, a more rigorous formulation of the bending angle has been investigated [8–15]. For instance, strong-field gravitational lensing in a Schwarzschild black hole was investigated by Frittelli, Kling and Newman [8], by Virbhadra and Ellis [9] and more comprehensively by Virbhadra [10]; distinctive lensing features of naked singularities were studied by many authors [11–20]. Kitamura, Nakajima and Asada proposed a lens model in the inverse powers of the distance as $1/r^n$ [21], such that the Schwarzschild lens, the Ellis wormhole lens and a gravitational lens associated with exotic matter (or energy) that might follow a non-standard equation of state can be discussed in a unified manner of describing these models as a one parameter family [22–25]. See also Tsukamoto et al. (2015) [26] for a possible connection between this inverse power model and the Tangherlini solution to the higher-dimensional Einstein equation.

Gibbons and Werner (2008) proposed an alternative way of deriving the deflection angle of light [27]. They used the Gauss-Bonnet theorem to a spatial domain described by the optical metric, where they assumed that the source and receiver are located at an asymptotic region. By extending Gibbons and Werner’s idea, Ishihara et al. have recently investigated finite-distance corrections [28]. However, such works [27, 28] are limited within the small

deflection limit.

Since the pioneering work by Darwin [29], on the other hand, the strong deflection limit has attracted a lot of interests (See e.g. [25, 30–32]), mainly because we expect that the recent progress in astronomical instruments will soon enable us to detect such strong deflection phenomena.

Therefore, the main purpose of the present paper is to extend the earlier work [28], especially in order to examine finite-distance corrections in the strong deflection limit. We shall discuss their implications for possible observations.

Throughout this paper, we use the unit of $G = c = 1$. In the following, the observer may be called the receiver in order to avoid a confusion between r_O and r_0 by using r_R .

II. GRAVITATIONAL DEFLECTION OF LIGHT AND GAUSS-BONNET THEOREM

A. Notation

Following Ishihara et al. [28], the present paper considers a static and spherically symmetric (SSS) spacetime. The SSS spacetime can be described as (cf. Eq.(23.3) in [5])

$$\begin{aligned} ds^2 &= g_{\mu\nu} dx^\mu dx^\nu \\ &= -A(r)dt^2 + B(r)dr^2 + C(r)d\Omega^2, \end{aligned} \tag{1}$$

where $d\Omega^2 \equiv d\theta^2 + \sin^2\theta d\phi^2$. This metric form allows us to consider a wormhole solution with a throat as well as a black hole spacetime. If we choose $C(r) = r^2$, then, r denotes the circumference radius. Without the loss of generality, henceforth, we choose the photon orbital plane as the equatorial plane ($\theta = \pi/2$). As usual, we define the impact parameter of the light ray as

$$\begin{aligned} b &\equiv \frac{L}{E} \\ &= \frac{C(r)}{A(r)} \frac{d\phi}{dt}, \end{aligned} \tag{2}$$

such that we can obtain the orbit equation as

$$\left(\frac{dr}{d\phi}\right)^2 + \frac{C(r)}{B(r)} = \frac{[C(r)]^2}{b^2 A(r) B(r)}. \tag{3}$$

Light rays satisfy the null condition as $ds^2 = 0$, which is rearranged as, via Eq. (1),

$$\begin{aligned} dt^2 &= \gamma_{IJ} dx^I dx^J \\ &= \frac{B(r)}{A(r)} dr^2 + \frac{C(r)}{A(r)} d\phi^2, \end{aligned} \quad (4)$$

where I and J denote 1 and 2. γ_{IJ} is called the optical metric. This optical metric defines a two-dimensional Riemannian space (denoted as M^{Opt}), in which the light ray is a spatial geodesic curve.

In M^{Opt} , let Ψ denote the angle of the light ray measured from the radial direction. We obtain

$$\cos \Psi = \frac{b\sqrt{A(r)B(r)} dr}{C(r) d\phi}, \quad (5)$$

which is rewritten in a more convenient form as

$$\sin \Psi = \frac{b\sqrt{A(r)}}{\sqrt{C(r)}}, \quad (6)$$

where we used Eq. (3).

Let Ψ_R and Ψ_S denote the angles that are measured at the receiver position (R) and the source position (S), respectively. Let $\phi_{RS} \equiv \phi_R - \phi_S$ denote the coordinate separation angle between the receiver and source. From the three angles Ψ_R , Ψ_S and ϕ_{RS} , let us define [28]

$$\alpha \equiv \Psi_R - \Psi_S + \phi_{RS}. \quad (7)$$

Eq.(7) has a geometrically invariant meaning as follows [28] .

Suppose that T is a two-dimensional orientable surface with boundaries ∂T_a ($a = 1, 2, \dots, N$) that are differentiable curves. See Figure 1. Let the jump angles between the curves be θ_a ($a = 1, 2, \dots, N$). Then, the Gauss-Bonnet theorem can be expressed as [33]

$$\iint_T K dS + \sum_{a=1}^N \int_{\partial T_a} \kappa_g d\ell + \sum_{a=1}^N \theta_a = 2\pi, \quad (8)$$

where K denotes the Gaussian curvature of the surface T , dS is the area element of the surface, κ_g means the geodesic curvature of ∂T_a , and ℓ is the line element along the boundary. The sign of the line element is chosen such that it is compatible with the orientation of the surface.

Let us consider a quadrilateral ${}_{R}^{\infty}\square_{S}^{\infty}$, which consists of the spatial curve for the light ray, two outgoing radial lines from R and from S and a circular arc segment C_r of coordinate radius r_C ($r_C \rightarrow \infty$) centered at the lens which intersects the radial lines through the receiver or the source. See Figure 2. Henceforth, we restrict ourselves within the asymptotically flat spacetime, for which $\kappa_g \rightarrow 1/r_C$ and $d\ell \rightarrow r_C d\phi$ as $r_C \rightarrow \infty$ (See e.g. [27]). Hence, $\int_{C_r} \kappa_g d\ell \rightarrow \phi_{RS}$. Applying this result to the Gauss-Bonnet theorem for ${}_{R}^{\infty}\square_{S}^{\infty}$, we obtain

$$\begin{aligned} \alpha &= \Psi_R - \Psi_S + \phi_{RS} \\ &= - \iint_{{}_{R}^{\infty}\square_{S}^{\infty}} K dS. \end{aligned} \quad (9)$$

Eq. (9) shows that α is invariant in differential geometry and α is well-defined even if L is a singularity point. Moreover, it follows that $\alpha = 0$ in Euclidean space.

Eq. (9) recovers the deflection angle of light in the far limit of the source and the receiver as

$$\alpha_{\infty} = 2 \int_0^{u_0} \frac{du}{\sqrt{F(u)}} - \pi, \quad (10)$$

where u is the inverse of r , u_0 is the inverse of the closest approach (often denoted as r_0) and $F(u)$ is defined as

$$F(u) \equiv \left(\frac{du}{d\phi} \right)^2, \quad (11)$$

which can be computed from Eq. (3).

Next, we consider another case that the distance from the source to the receiver is finite because every observed stars and galaxies are located at finite distance from us (e.g., at finite redshift in cosmology) and the distance is much larger than the size of the lens. Let u_R and u_S denote the inverse of r_R and r_S , respectively, where r_R and r_S are finite. Eq. (7) becomes [28]

$$\alpha = \int_{u_R}^{u_0} \frac{du}{\sqrt{F(u)}} + \int_{u_S}^{u_0} \frac{du}{\sqrt{F(u)}} + \Psi_R - \Psi_S. \quad (12)$$

III. EXTENSION TO A STRONG DEFLECTION LIMIT

In the previous section for the weak deflection, a spatial curve from the source to the receiver is simple. In the strong deflection limit, however, a spatial curve from the source to the receiver may have a winding number that can exceed unity. Therefore, the spatial curve

may have intersection points. We split the curve into pieces, such that each of the pieces can have no intersection.

A. Loops of the curve for the photon orbit

We begin with the case of one loop for its simplicity. Please see Figure 3. First, we examine the two quadrilaterals (1) and (2) in Figure 4, which can be constructed by imagining an auxiliary point (P) that may be the periastron and then by assuming auxiliary outgoing radial lines (solid line in the figure) from the point P in the quadrilaterals (1) and (2). In fact, it does not matter that the point P is chosen as the periastron. Note that the direction of the two auxiliary lines in (1) and (2) is opposite and thus the two auxiliary lines cancel out to make no contributions to α in the sum of the quadrilaterals (1) and (2). Let θ_1 and θ_2 denote the inner angle at the point P in the quadrilateral (1) and that in the quadrilateral (2), respectively. We find $\theta_1 + \theta_2 = \pi$, because the line from the source to the receiver is a geodesic curve and the point P lies on the geodesic.

For each orientable quadrilateral in Figure 4, the method in the previous section can be applied as it is. In the similar manner to deriving Eq. (9), we obtain

$$\begin{aligned}\alpha^{(1)} &= (\pi - \theta_1) - \Psi_S + \phi_{RS}^{(1)}, \\ \alpha^{(2)} &= \Psi_R - \theta_2 + \phi_{RS}^{(2)},\end{aligned}\tag{13}$$

where the coordinate angle difference ϕ_{RS} is split into two parts, $\phi_{RS}^{(1)}$ for the quadrilateral (1) and $\phi_{RS}^{(2)}$ for the other quadrilateral (2).

If $r_S = r_R$, then, there is a reflection symmetry between the quadrilaterals (1) and (2) and $\phi_{RS}^{(1)} = \phi_{RS}^{(2)} = \phi_{RS}/2$. Otherwise, $\phi_{RS}^{(1)}$ does not always equal to $\phi_{RS}^{(2)}$. In any case, however, $\phi_{RS}^{(1)} + \phi_{RS}^{(2)} = \phi_{RS}$. Ψ_S and $(\pi - \Psi_R)$ are the inner angles at S and R , respectively, where we should remember that Ψ_R is an angle measured from the outgoing radial line. We thus obtain

$$\begin{aligned}\alpha &= \alpha^{(1)} + \alpha^{(2)} \\ &= \Psi_R - \Psi_S + \phi_{RS},\end{aligned}\tag{14}$$

where we use $\theta_1 + \theta_2 = \pi$ and $\phi_{RS}^{(1)} + \phi_{RS}^{(2)} = \phi_{RS}$. This result takes the same form as Eq. (7), but we should note that it is derived for one loop case.

Next, we consider a case of two loops as shown by Figure 5, for which we draw auxiliary lines to split the configuration into four quadrilaterals (See Figure 6). For each quadrilateral, we obtain

$$\begin{aligned}
\alpha^{(1)} &= (\pi - \theta_1) - \Psi_S + \phi_{RS}^{(1)}, \\
\alpha^{(2)} &= (\pi - \theta_3) - \theta_2 + \phi_{RS}^{(2)}, \\
\alpha^{(3)} &= (\pi - \theta_5) - \theta_4 + \phi_{RS}^{(3)}, \\
\alpha^{(4)} &= \Psi_R - \theta_6 + \phi_{RS}^{(4)},
\end{aligned} \tag{15}$$

where $\phi_{RS}^{(1)} + \phi_{RS}^{(2)} + \phi_{RS}^{(3)} + \phi_{RS}^{(4)} = \phi_{RS}$. We thus obtain

$$\begin{aligned}
\alpha &= \alpha^{(1)} + \alpha^{(2)} + \alpha^{(3)} + \alpha^{(4)} \\
&= \Psi_R - \Psi_S + \phi_{RS},
\end{aligned} \tag{16}$$

where we use $\theta_1 + \theta_2 = \theta_3 + \theta_4 = \theta_5 + \theta_6 = \pi$. While Eq. (16) is derived for the two-loop case, it reveals again the form of Eq. (7). Note that one loop, from which the quadrilaterals (2) and (3) can be constructed, makes the contribution to α only in terms of $\phi_{RS}^{(2)} + \phi_{RS}^{(3)}$.

Finally, we consider any winding number W . We construct $2W$ quadrilaterals, for which the inner angles at finite distance from L are denoted as $\theta_0, \dots, \theta_{2W}$ in order from S to R . Here, $\theta_0 = \Psi_S$ and $\theta_{2W} = \pi - \Psi_R$. See Figure 7 for one of the quadrilaterals. Any pair of neighboring quadrilaterals (N) and (N+1) makes the contribution to α only by $\phi_{RS}^{(N)} + \phi_{RS}^{(N+1)}$, because $\theta_{2N-1} + \theta_{2N} = \theta_{2N+1} + \theta_{2N+2} = \pi$ and the auxiliary lines cancel out. By induction, therefore, Eq. (7) can be derived for any winding number.

Eq. (7), which is equivalent to Eq. (12) by using the orbit equation, is rearranged as

$$\begin{aligned}
\alpha &= \Psi_R - \Psi_S + \phi_{RS} \\
&= \Psi_R - \Psi_S + \int_{u_R}^0 \frac{du}{\sqrt{F(u)}} + \int_{u_S}^0 \frac{du}{\sqrt{F(u)}} + 2 \int_0^{u_0} \frac{du}{\sqrt{F(u)}}.
\end{aligned} \tag{17}$$

The finite-distance correction to the deflection angle of light, denoted as $\delta\alpha$, is the difference between the asymptotic deflection angle and the deflection angle for the finite distance case. It is expressed as

$$\delta\alpha = \alpha - \alpha_\infty. \tag{18}$$

Substituting Eqs. (10) and (17) into the right-hand side of Eq. (18) and rearranging it, we obtain

$$\delta\alpha = (\Psi_R - \Psi_S + \pi) + \int_{u_R}^0 \frac{du}{\sqrt{F(u)}} + \int_{u_S}^0 \frac{du}{\sqrt{F(u)}}. \quad (19)$$

This expression suggests two origins of the finite-distance corrections. One origin is the angles Ψ_R and Ψ_S that are defined at the receiver and the source at finite distance, where the space is non-Euclidean [34]. The other origin is the two path integrals, one from the receiver position to the spatial infinity and the other from the source to the infinity. Therefore, if both the receiver and the source are in the weak field region as is common in astronomy, the finite-distance correction comes only from the weak field region but not from the strong field region, even if the light ray passes near the photon sphere ($r_0 \sim r_{ph}$), where r_{ph} denotes the photon sphere radius. This is quite reasonable.

B. Approximations

As a concrete example, henceforth, we focus on the Schwarzschild black hole with mass M . Then, Eq. (11) becomes

$$F(u) = \frac{1}{b^2} - u^2 + 2Mu^3. \quad (20)$$

Eq. (17) with $F(u)$ given by Eq. (20) can be solved analytically but leads to cumbersome expressions involving incomplete elliptic integrals of the first kind. In the case that the source and the receiver are far from the lens ($r_S \gg b, r_R \gg b$) but the light ray passes near the photon sphere ($r_0 \sim 3M$), Eq. (17) can be approximated and simplified considerably as

$$\begin{aligned} \alpha = & \frac{2M}{b} \left[\sqrt{1 - b^2 u_R^2} + \sqrt{1 - b^2 u_S^2} - 2 \right] \\ & + 2 \log \left(\frac{12(2 - \sqrt{3})r_0}{r_0 - 3M} \right) - \pi \\ & + O \left(\frac{M^2}{r_R^2}, \frac{M^2}{r_S^2}, 1 - \frac{3M}{r_0} \right), \end{aligned} \quad (21)$$

where the logarithmic term [31] was used for the last term of Eq. (17). Here, the leading terms in Ψ_R and Ψ_S cancel out with the terms Ψ coming from the integrals. Therefore, Ψ_R and Ψ_S do not appear in the final expression of Eq. (21). See Appendix for more details.

As stated above, it is natural that the logarithmic term due to the strong field is independent of finite-distance corrections such as a multiplication by $\sqrt{1 - (bu_S)^2}$. By chance,

$\delta\alpha$ for the strong deflection limit (See Eq. (17)) is the same as that for the weak deflection case (See e.g. Eq. (29) in [28]). This suggests that the finite-distance correction for the strong deflection limit is of the same order as

$$\delta\alpha \sim O\left(\frac{Mb}{r_S^2} + \frac{Mb}{r_R^2}\right), \quad (22)$$

for the weak field case (e.g. [28]). Namely, the correction is linear in the impact parameter. This implies that the finite-distance correction for the weak deflection case (large b) is larger than that in the strong deflection limit (small b), if the other parameters are fixed. In the next section, we shall discuss in more detail.

IV. POSSIBLE OBSERVATIONAL CANDIDATES

A. Gravitational bending of light by the Sun

We assume that an observer at the Earth sees the light bending by the solar mass, while the source is practically at the asymptotic region. If the light ray passes near the solar surface, Eq. (22) implies that the finite-distance correction to this case is of the order of

$$\begin{aligned} \delta\alpha &\sim \frac{Mb}{r_R^2} \\ &\sim 10^{-5} \text{arcsec.} \times \left(\frac{M}{M_\odot}\right) \left(\frac{b}{R_\odot}\right) \left(\frac{1\text{AU}}{r_R}\right)^2, \end{aligned} \quad (23)$$

where $4M_\odot/R_\odot \sim 1.75 \text{ arcsec.}$, and R_\odot denotes the solar radius. Note that Eq. (23) comes from Eq. (29) in Ref. [28] for the weak-field limit and therefore it is independent of Eq. (21) for the strong deflection limit.

This correction of $\sim 10^{-5} \text{ arcsec.}$ (= 10 micro arcseconds), is close to the angular accuracy within the capability of near-future astronomy. For instance, a current astrometry space mission Gaia [35] and a future one JASMINE (Japan Astrometry Satellite Mission for Infrared Exploration) [36] are expected to approach nearly ten micro arcseconds, though the solar direction is too bright and even dangerous for these telescopes. In order to measure the above finite-distance correction, a specially dedicated instrument such as a corona graph might be needed or a total solar eclipse for an astrometry satellite could be used along the original idea by Arthur Eddington.

Figure 8 shows numerical calculations of the bending angle of light due to the finite distance of the receiver. These analytic and numerical results, Eq. (23) and Figure 8, are consistent with each other and they suggest that $\delta\alpha$ by the solar mass might not be negligible in future astrometry observations. Note that the above correction happens to be comparable to the deflection of light at the second post-Newtonian order. If a 2PN test of the light bending by the Sun is done in the future, therefore, the above correction might be relevant.

B. Sgr A*

Next, we consider the strong deflection limit. One of the most plausible candidates for the strong deflection is at the center of our Galaxy. It is identified with Sgr A*. In this case, the receiver distance is much larger than the impact parameter of light, while a source star may be in the central region of our Galaxy.

For Sgr A*, Eq. (22) implies

$$\begin{aligned} \delta\alpha &\sim \frac{Mb}{r_S^2} \\ &\sim 10^{-5} \text{arcsec.} \times \left(\frac{M}{4 \times 10^6 M_\odot} \right) \left(\frac{b}{3M} \right) \left(\frac{0.1 \text{pc}}{r_S} \right)^2, \end{aligned} \quad (24)$$

where we assume the mass of the central black hole as $M \sim 4 \times 10^6 M_\odot$ and the strong deflection limit as $b \sim 3M$. This angle might be reachable in near-future astronomy.

Please see Figure 9 for numerical calculations of the finite-distance correction due to the source location. This figure and also Eq. (24) suggest that $\delta\alpha$ can be of the order of ten (or more) micro arcseconds, if a source star is sufficiently close to Sgr A*, for instance within a tenth of one parsec from Sgr A*. In other words, for such a close source case, even though the source is still in the weak field, the infinite-distance limit is no longer sufficient. We have to take account of finite-distance corrections that are proposed in this paper.

V. CONCLUSION

For a static, spherically symmetric and asymptotically flat spacetime, we used the Gauss-Bonnet theorem to show that Eq. (17) gives the exact bending angle of light especially by taking account of the finite distance from a lens object to a light source and a receiver,

such that the definition can be valid also in the strong deflection limit. Finally, this method was applied to Schwarzschild spacetime as a concrete example. We discussed also possible observational implications. The proposed finite-distance corrections for Sgr A* for instance are able to amount to $\sim 10^{-5}$ arcseconds for a limited parameter range, which may be within the scope of near-future astronomy. Also the finite-distance correction to the Sun is $\sim 10^{-5}$ arcseconds, while this case is in the weak-field limit.

It would be interesting to apply Eq. (18) or Eq. (19) to other black hole models and then to study a relation with future observations. It is left for future work.

Acknowledgments

We are grateful to Marcus Werner for the stimulating discussions, especially for his useful comments on their approach based on the Gauss-Bonnet theorem. We wish to thank Makoto Sakaki for giving us the useful literature information on the Gauss-Bonnet theorem. We would like to thank Toshifumi Futamase, Masumi Kasai, Yuuiti Sendouda, Ryuichi Takahashi, Atushi Naruko, Yuya Nakamura and Naoki Tsukamoto for the useful conversations. We would like to thank Hideki Ishihara for his hospitality at JGRG26 (The 26th Workshop on General Relativity and Gravitation in Japan) in Osaka, where this work was largely developed. This work was supported in part by Japan Society for the Promotion of Science Grant-in-Aid for Scientific Research, No. 26400262 (H.A.) and in part by by Ministry of Education, Culture, Sports, Science, and Technology, No. 15H00772 (H.A.).

Appendix A: Derivation of Eq. (21)

While the light ray passes near the photon sphere ($r_0 \sim 3M$), we assume that the receiver and the source are very far from the lens ($r_R \gg r_0$ and $r_S \gg r_0$). Straightforward calculations for the Schwarzschild case give

$$\begin{aligned} \Psi_R - \Psi_S = & \arcsin(bu_R) + \arcsin(bu_S) - \pi \\ & - \frac{Mbu_R^2}{\sqrt{1-b^2u_R^2}} - \frac{Mbu_S^2}{\sqrt{1-b^2u_S^2}} + O\left(\frac{M^2}{r_R^2}, \frac{M^2}{r_S^2}\right), \end{aligned} \quad (\text{A1})$$

$$\begin{aligned}
\int_{u_R}^0 \frac{du}{\sqrt{F(u)}} + \int_{u_S}^0 \frac{du}{\sqrt{F(u)}} &= -\arcsin(bu_R) + \frac{2M}{b\sqrt{1-b^2u_R^2}} \left(1 - \frac{1}{2}b^2u_R^2\right) \\
&\quad -\arcsin(bu_S) + \frac{2M}{b\sqrt{1-b^2u_S^2}} \left(1 - \frac{1}{2}b^2u_S^2\right) \\
&\quad -\frac{4M}{b} + O\left(\frac{M^2}{r_R^2}, \frac{M^2}{r_S^2}\right),
\end{aligned} \tag{A2}$$

and

$$2 \int_0^{u_0} \frac{du}{\sqrt{F(u)}} = 2 \log\left(\frac{12(2-\sqrt{3})r_0}{r_0-3M}\right) + O\left(1 - \frac{3M}{r_0}\right), \tag{A3}$$

where we use Eqs. (6) and (20). Eq. (A3) was derived by Iyer and Petters [31]. By substituting Eqs. (A1)-(A3) into Eq. (17), we obtain Eq. (21). Note that $\arcsin(bu_R)$ and $\arcsin(bu_S)$, which are the leading terms of Ψ_R and Ψ_S , cancel out with the terms in the path integrals of Eq. (A2). Therefore, $\arcsin(bu_R)$ and $\arcsin(bu_S)$ do not appear in Eq. (21), while Ψ_R and Ψ_S do contribute to α .

-
- [1] F. W. Dyson, A. S. Eddington, C. Davidson, *Phil. Trans. R. Soc. A* **220**, 291 (1920).
 - [2] A. Einstein, *Ann. Phys. (Berlin)* **49**, 769 (1916).
 - [3] Y. Hagihara, *Jpn. J Astron. Geophys.* **8**, 67 (1931).
 - [4] S. Chandrasekhar, *The Mathematical Theory of Black Holes*, (Oxford University Press, New York, 1998).
 - [5] C. W. Misner, K. S. Thorne, J. A. Wheeler, *Gravitation*, (Freeman, New York, 1973).
 - [6] V. A. Brumberg, *Essential relativistic celestial mechanics*, (Bristol, UK: Adam Hilger, 1991).
 - [7] S. Zschocke, *Class. Quantum Grav.* **28**, 125016 (2011).
 - [8] S. Frittelli, T. P. Kling, and E. T. Newman, *Phys. Rev. D* **61**, 064021 (2000).
 - [9] K. S. Virbhadra, and G. F. R. Ellis, *Phys. Rev. D* **62**, 084003 (2000).
 - [10] K. S. Virbhadra, *Phys. Rev. D* **79**, 083004 (2009).
 - [11] K. S. Virbhadra, D. Narasimha, and S. M. Chitre, *Astron. Astrophys.* **337**, 1 (1998).
 - [12] K. S. Virbhadra, and G. F. R. Ellis, *Phys. Rev. D* **65**, 103004 (2002).
 - [13] K. S. Virbhadra, and C. R. Keeton, *Phys. Rev. D* **77**, 124014 (2008).
 - [14] E. F. Eiroa, G. E. Romero, and D. F. Torres, *Phys. Rev. D* **66**, 024010 (2002).
 - [15] V. Perlick, *Phys. Rev. D* **69**, 064017 (2004).

- [16] J. P. DeAndrea, and K. M. Alexander, Phys. Rev. D **89**, 123012 (2014).
- [17] F. Abe, Astrophys. J. **725**, 787 (2010).
- [18] Y. Toki, T. Kitamura, H. Asada, and F. Abe, Astrophys. J. **740**, 121 (2011).
- [19] K. Nakajima, and H. Asada, Phys. Rev. D **85**, 107501 (2012).
- [20] G. W. Gibbons, and M. Vyska, Class. Quant. Grav. **29** 065016 (2012).
- [21] T. Kitamura, K. Nakajima, and H. Asada, Phys. Rev. D **87**, 027501 (2013).
- [22] K. Izumi, C. Hagiwara, K. Nakajima, T. Kitamura, and H. Asada, Phys. Rev. D **88**, 024049 (2013).
- [23] T. Kitamura, K. Izumi, K. Nakajima, C. Hagiwara, and H. Asada, Phys. Rev. D **89**, 084020 (2014).
- [24] K. Nakajima, K. Izumi, and H. Asada, Phys. Rev. D **90**, 084026 (2014).
- [25] N. Tsukamoto, and T. Harada, Phys. Rev. D **87**, 024024 (2013).
- [26] N. Tsukamoto, T. Kitamura, K. Nakajima, and H. Asada, Phys. Rev. D **90**, 064043 (2014).
- [27] G. W. Gibbons, and M. C. Werner, Class. Quant. Grav. **25**, 235009 (2008).
- [28] A. Ishihara, Y. Suzuki, T. Ono, T. Kitamura, and Hideki Asada, Phys. Rev. D **94**, 084015 (2016).
- [29] C. Darwin, Proc. R. Soc. A **249**, 180 (1959).
- [30] V. Bozza, Phys. Rev. D **66**, 103001 (2002).
- [31] S. V. Iyer and A. O. Petters, Gen. Relativ. Gravit. **39**, 1563 (2007).
- [32] V. Bozza, and G. Scarpetta, Phys. Rev. D **76**, 083008 (2007).
- [33] M. P. Do Carmo, *Differential Geometry of Curves and Surfaces*, pages 268-269, (Prentice-Hall, New Jersey, 1976).
- [34] In the present paper, we use the optical metric for suitably defining the angle in M^{opt} . On the other hand, Bozza and Scarpetta [32] did not take care of this matter and they used the spatial part of the spacetime metric for its simplicity.
- [35] <http://sci.esa.int/gaia/>
- [36] <http://www.jasmine-galaxy.org/index-en.html>

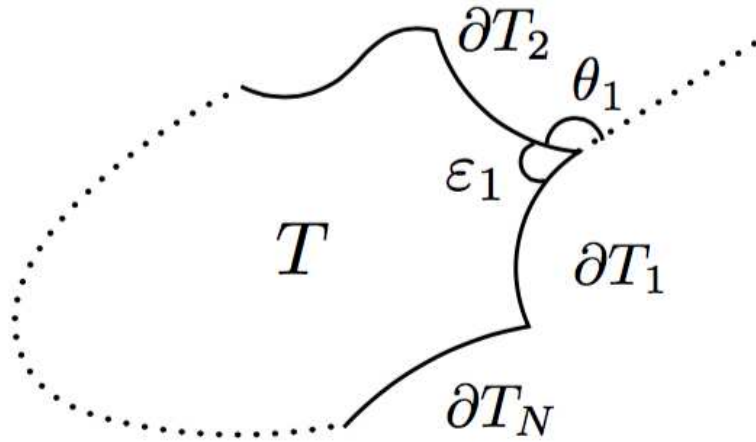


FIG. 1: Schematic figure for the Gauss-Bonnet theorem.

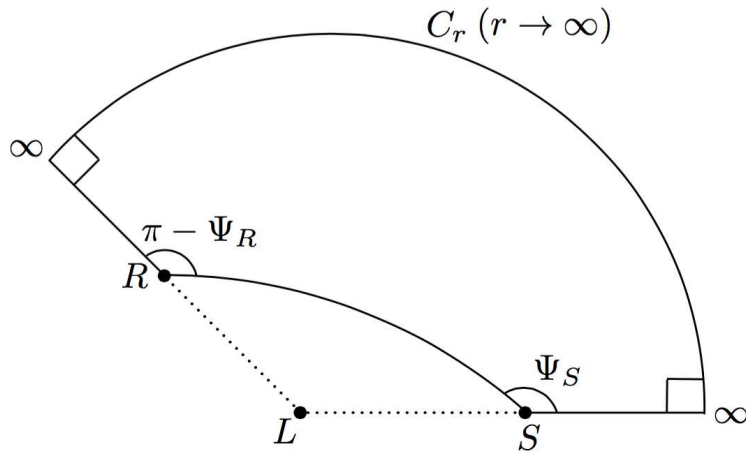


FIG. 2: Quadrilateral $\infty_R \square_S^\infty$ embedded in a curved space in M^{opt} .

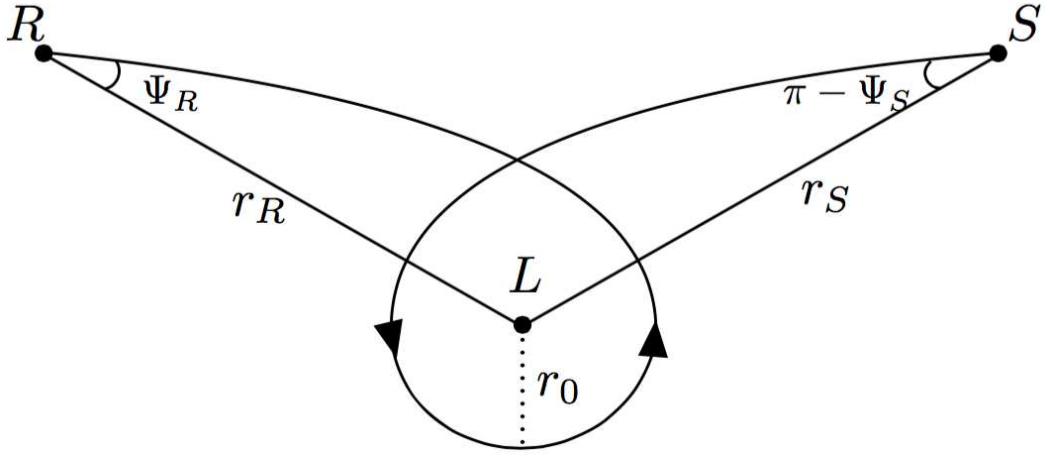


FIG. 3: One-loop diagram for the photon trajectory in M^{opt} .

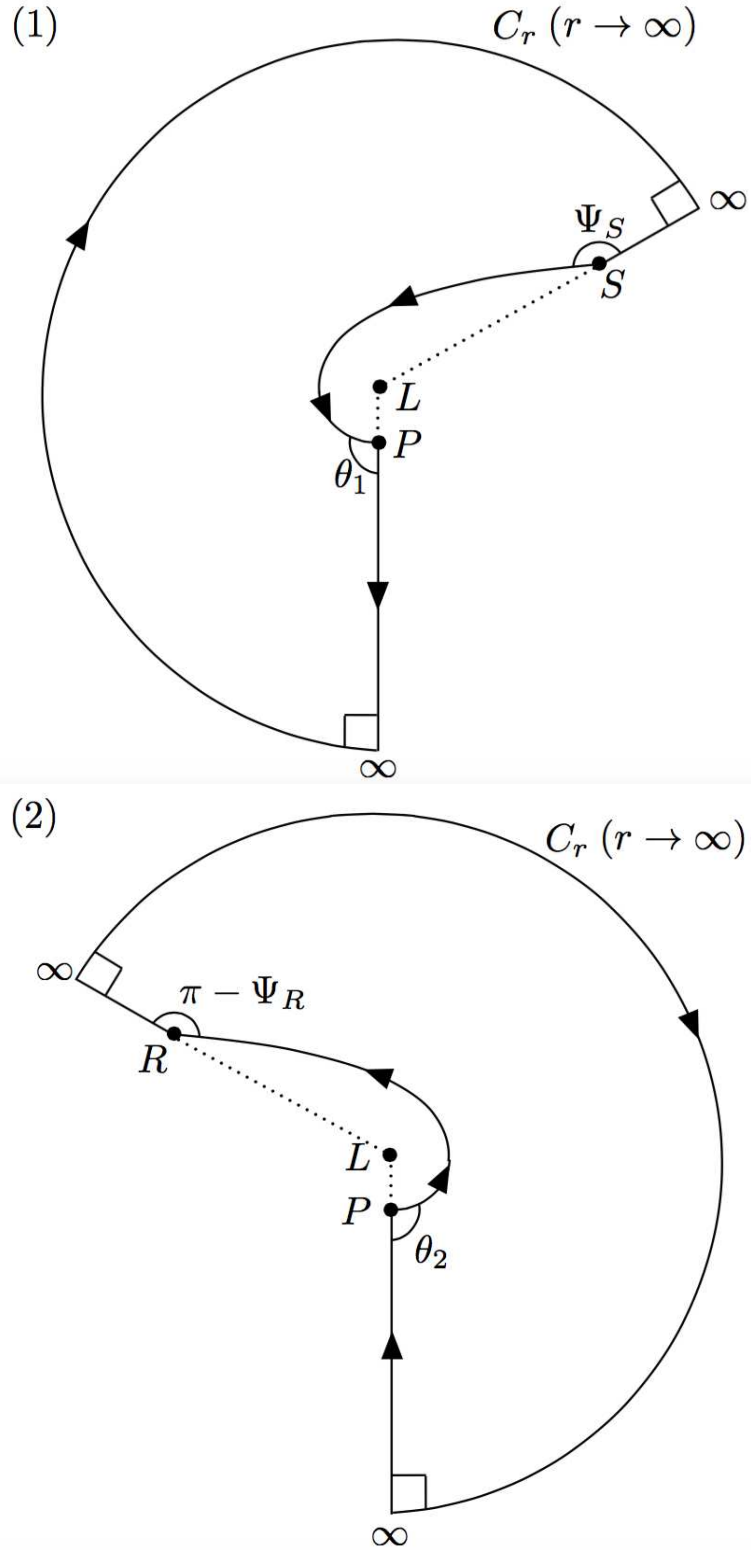


FIG. 4: Two quadrilaterals from the photon orbit in Figure 3. They are embedded in a non-Euclidean space.

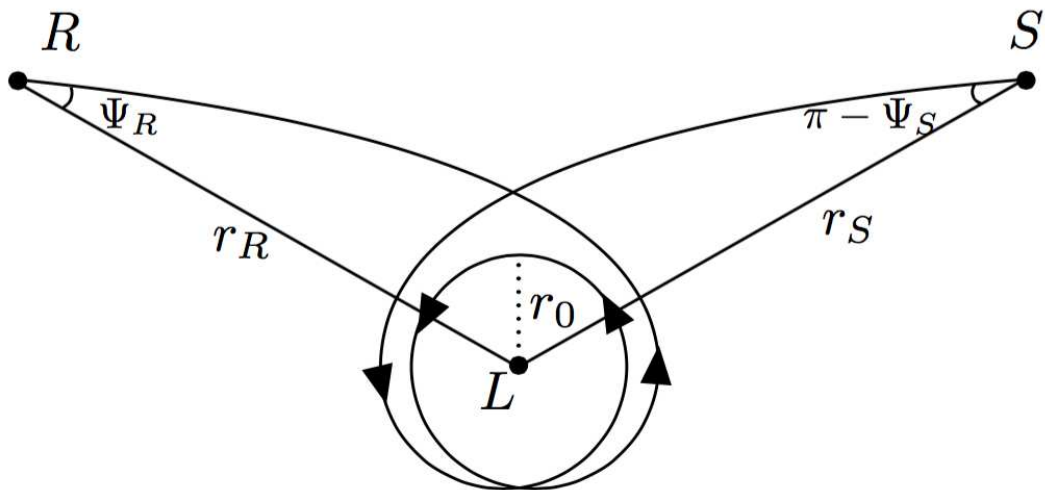


FIG. 5: Two-loop diagram for the photon trajectory in M^{opt} .

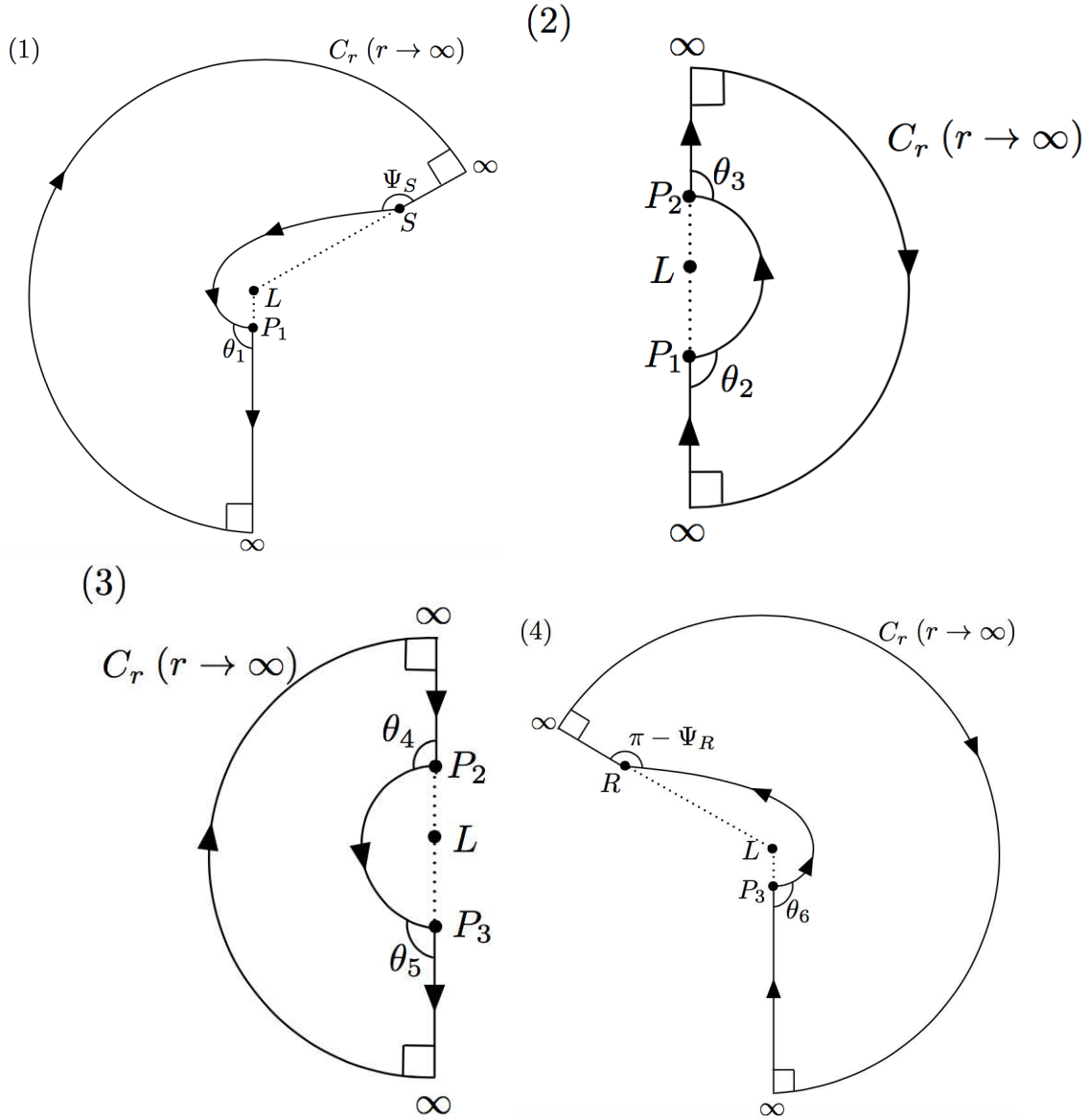


FIG. 6: Four quadrilaterals (1)-(4) in a non-Euclidean space M^{opt} . They are constructed from the two-loop diagram for the photon orbit in Figure 5.

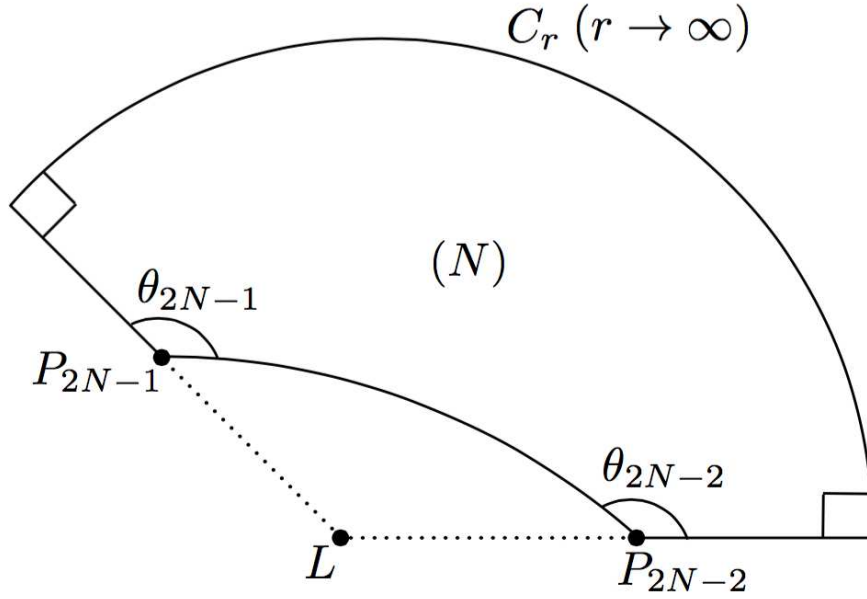


FIG. 7: One of quadrilaterals from a photon orbit with any winding number. This can be used in order to prove by induction that Eq. (7) holds for any loop number case.

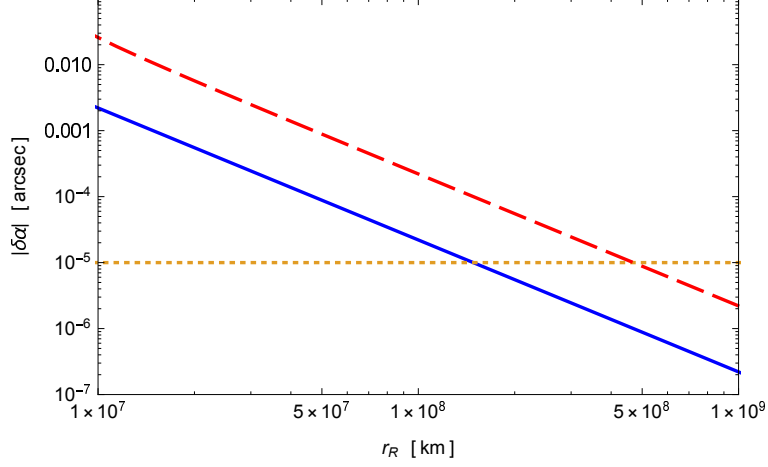


FIG. 8: $\delta\alpha$ given by Eq. (23) for the Sun. The vertical axis denotes the finite-distance correction to the deflection angle of light and the horizontal axis denotes the receiver distance r_R . The solid curve (blue in color) and dashed one (red in color) correspond to $b = R_\odot$ and $b = 10R_\odot$, respectively. The dotted line (yellow in color) corresponds to 10 micro arcseconds.

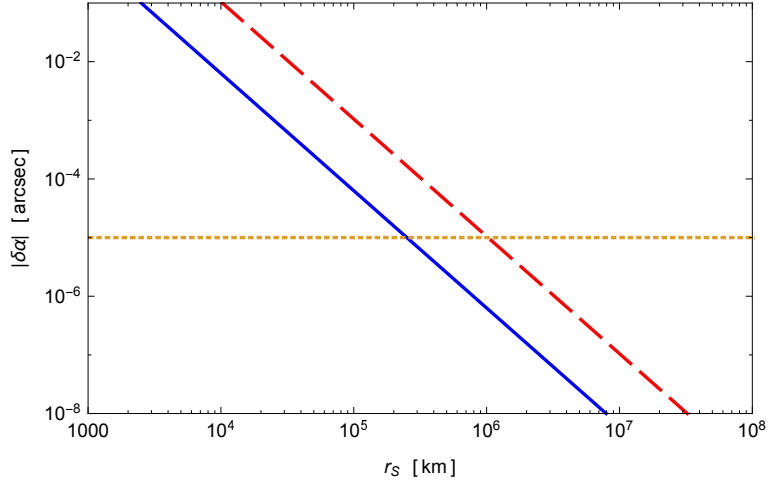


FIG. 9: $\delta\alpha$ given by Eq. (24) for the Sgr A*. The vertical axis denotes the finite-distance correction to the deflection angle of light and the horizontal axis denotes the source distance r_S . The solid curve (blue in color) and dashed one (red in color) correspond to $b = 6M$ and $b = 10^2M$, respectively. The dotted line (yellow in color) corresponds to 10 micro arcseconds.